Arabian Journal of Geosciences (2020) 13: 1243
https://doi.org/10.1007/s12517-020-06240-7

ORIGINAL PAPER

Uniaxial compression creep and acoustic emission characteristics of sandstone under loading-unloading paths

Kui Zhao[1] · Liangxiao Xiong[2,3] · Yangdong Xu[1] · Zhongyuan Xu[4] · Peng Zeng[1]

Received: 10 November 2019 / Accepted: 10 November 2020 / Published online: 20 November 2020

Abstract
Specimens of red sandstone are subjected to creep and acoustic emission (AE) tests under only multi-level loading and multi-level loading-unloading. Creep deformation characteristics and AE parameters of the red sandstone specimens under these two loading paths are compared and analyzed, and a creep AE damage-variable model is used for the damage evolution of the micro-cracked structures inside the rock during the creep process. The research results reveal the following: (1) During the creep process involving multi-level loading-unloading, the temporal variation of the AE amplitude is similar to that observed during the creep process involving only multi-level loading. (2) The variations of the cumulative AE event and cumulative AE ring-down count in the creep process involving multi-level loading-unloading are similar to those in the creep process involving only multi-level loading, while the actual values are higher in the former process. (3) The creep AE damage-variable model performs well on characterizing the damage evolution of the internal micro-crack structure of the rock in both creep processes.

Keywords Red sandstone · Uniaxial compression-creep test · Multi-level loading-unloading · Acoustic emission characteristics · Damage variable

Introduction

Rock creep indicates the deformation characteristics of rock under constant load, and it is different from rock characteristics under static loading and dynamic loading (Kong et al. 2020). Creep significantly affects the stability of engineering rock masses.

Many experimental studies investigated the compression-creep properties of rock, and most researchers used multi-level loading when conducting such tests. However, the excavation and support can either increase or decrease the stress in the surrounding rock during underground engineering. Therefore, in compression-creep tests, multi-level loading is inconsistent with the manner in which stress changes in the surrounding rock. Instead, multi-level loading-unloading is used to conduct rock compression-creep tests in this study, which is more consistent with how stress changes in the surrounding rock during underground engineering.

Compare to multi-level loading tests, relatively fewer researchers have used multi-level loading-unloading in

Responsible Editor: Zeynal Abiddin Erguler

✉ Liangxiao Xiong
xionglx1982@126.com

Kui Zhao
296931654@qq.com

Yangdong Xu
1253103753@qq.com

Zhongyuan Xu
zyxu@udel.edu

Peng Zeng
402230385@qq.com

[1] School of Resources & Environment Engineering, Jiangxi University of Science and Technology, Ganzhou 341000, Jiangxi Province, China

[2] School of Civil Engineering and Architecture, East China Jiaotong University, Nanchang 330013, China

[3] Guangxi Key Laboratory of Disaster Prevention and Engineering Safety, Guangxi University, Nanning 530004, China

[4] Department of Earth Sciences, University of Delaware, Newark, DE 19716, USA

compression-creep tests. Zhao et al. (2009) conducted viscoelastic/plastic-creep experiments on soft ore rock under circular incremental loading-unloading and found that soft rocks enhance ability to resist instantaneous elastic deformation and instantaneous plastic deformation during the multi-level loading-unloading in the cyclic process. Yang et al. (2014a) conducted large-scale in situ compressive-creep tests on the weak layer using a rigid bearing plate and loading-unloading cycles and expressed that the five-parameter generalized Kelvin model is a good representation of the creep behavior of the weak rock layer. Yang et al. (2015) performed triaxial compression experiments on deeply buried marble specimens to investigate their short-term and creep behavior under cyclic loading and pointed out that the steady-state creep rate of marble increases nonlinearly with the increasing axial deviatoric stress. Zhao et al. (2017a) carried out a series of triaxial creep tests on intact and cracked Maokou limestone specimens under multi-level loading-unloading cycles and found that the viscoelastic strain converges to a certain value with time, but the viscoplastic strain keeps increasing with time. Zhao et al. (2017b) presented an extensive laboratory investigation of the nonlinear rheological mechanical characteristics of hard rock under cyclic incremental loading-unloading and found that the proportion of instantaneous plastic strain to total instantaneous strain has an increasing tendency with higher deviatoric stress overall. Similarly, relatively few researchers have used unloading confining stress when conducting compression-creep tests. Huang et al. (2017) conducted triaxial unloading confining pressure creep tests on sandy mudstone specimens to study the dilatancy and fracturing behavior of soft rock. They revealed that when the deviatoric stress is larger and the experienced creep time is longer, the unloading effect and creep characteristics are more apparent and are accompanied by more obvious lateral dilatancy. Hu et al. (2019) performed cyclic loading-unloading creep experiments on the artificial layered cemented specimens with various layer angles. They showed that time-independent strains have linear correlations with the applied stress ratio, whereas time-dependent strains have nonlinear correlations with the stress ratio.

When rock material is subjected to an external load, expansion of internal micro-cracks and friction between particles both act as ready sources of acoustic emission (AE). Recently, many tests have been conducted on rock AE. Yang et al. (2014b) conducted multi-stage triaxial compression tests on cylindrical red sandstone specimens and displayed that the spatial AE events are not active and distribute stochastically in the specimen before peak strength, while after peak strength, the spatial AE events are very active and focus on a local region beyond final microscopic failure plane. Kim et al. (2015) found that the AE energy and damage parameter from the moment tensor of granite are very close not only on the stress thresholds of crack initiation and crack damage but also close on the patterns of progressive damage evolution. Zhang et al. (2015) pointed out that the AE activity and energy release of rock salt with coarse grains and non-uniform structures decrease with increasing stress level. Meng et al. (2016) found that the acoustic emission intensity of rock specimens during uniaxial cyclic loading-unloading compression changes repeatedly. Wang et al. (2019) showed that the peak AE activity of saturated karst limestone under uniaxial compression occurs near the peak stress of the rock. Meng et al. (2018) found that the AE characteristics are closely related to the stress-strain properties of rock materials and are affected by the developmental stage and degree of internal micro-cracks. Zhang et al. (2018) divided the AE energy curves of anisotropic coal under triaxial stress into three types: rapid facture type, stable fracture type, and plastic fracture type.

Because rock creep takes a relatively long time and involves a relatively complex failure mechanism, few studies about rock creep AE exist currently, especially regarding the analysis and investigation of AE characteristics during rock creep process under different loading modes.

Therefore, in the present study, we conduct creep-AE tests and theoretical analysis on red sandstone under multi-level loading-unloading. We experimentally obtain the creep-AE characteristics of the rock during (i) multi-level loading and (ii) multi-level loading-unloading; those characteristics include AE amplitude, cumulative AE event, and cumulative AE ring-down count.

Test equipment, specimen characteristics, and experimental groups

Test equipment

The creep-AE test equipment used in the present study comprises two main parts, namely, a triaxial rheological testing machine (HPTAS; GDS Instruments, UK) and an AE system as shown in Fig. 1. The uniaxial compression-creep tests were conducted on the triaxial rheological testing machine with a maximum axial load of 400 kN. The AE system is composed of an AE acquisition board (PCI-2; Physical Acoustics, USA) and control software (AEwin; Physical Acoustics).

Specimen characteristics and experimental groups

The red sandstone specimens used in present experiments were obtained from the south of Jiangxi Province in China. After processing, the rock specimens were dried naturally under the same conditions. In the meantime, in order to keep a high requirement, the specimens with obvious cracks on the surface were removed, and then the sonic test was used to screen out the rock specimens with uniform integrity and homogeneity. Finally, we selected 13 representative specimens for the uniaxial compression test and uniaxial compression-creep test in this study. These 13 representative cylindrical specimens are shown in Fig. 2.

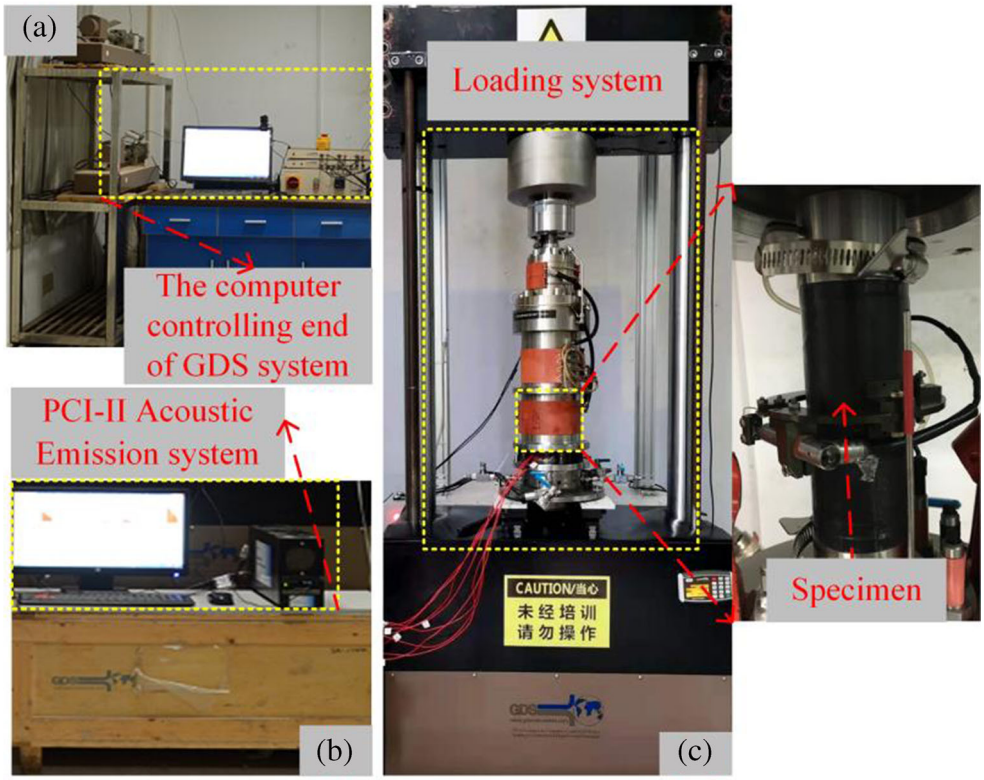

Fig. 1 Triaxial rheological testing machine and AE system

Uniaxial compression tests

We conducted uniaxial compression tests on the five specimens (HR-9#, HR-10#, HR-11#, HR-12#, and HR-13#). The uniaxial compressive strength of the present red sandstone is 27–35 MPa with an average of 30.48 MPa. This average uniaxial compressive strength provided the test basis for the loading control of the creep-AE tests under loading-unloading.

Tests of uniaxial compression creep and acoustic emission characteristics

We tested four specimens (HR-5#, HR-6#, HR-7#, and HR-8#) for their creep-AE characteristics under multi-level loading and other four specimens (HR-1#, HR-2#, HR-3#, and HR-4#) for their creep-AE characteristics under multi-level loading-unloading. The test parameters of all the specimens are listed in Table 1.

Fig. 2 Processed red sandstone specimens

Loading methods of creep tests

The loading methods used in the present creep tests are multi-level loading and multi-level loading-unloading. Based on the average uniaxial compressive strength of the red sandstone specimens, the creep tests were divided into 10 different stress levels, and the corresponding load of each stage is 10 kN, 15 kN, 20 kN, 25 kN, 30 kN, 35 kN, 40 kN, 45 kN, 50 kN, and 55 kN. The first and tenth stresses are approximately 16% and 85%, respectively, of the average uniaxial compressive strength of the red sandstone specimens.

Creep tests: multi-level loading

During the creep tests, the axial stress was increased incrementally from low to high. Each stage of the load was increased to the next stage after completion of the predetermined time until the final level of stress was reached. During this process, the AE monitoring was synchronized with the compression-creep test.

Table 1 Test parameters of all the specimens

Test type	Specimen no.	Specimen size		Peak stress (MPa)
		Diameter (mm)	Height (mm)	
Multi-level loading-unloading creep test	HR-1#	49.30	99.52	28.83
	HR-2#	49.10	100.04	18.49
	HR-3#	49.30	98.80	31.45
	HR-4#	48.90	98.00	29.30
Multi-level loading creep test	HR-5#	49.40	98.90	31.32
	HR-6#	48.60	98.20	32.36
	HR-7#	48.30	99.90	27.30
	HR-8#	48.20	99.50	30.16
Uniaxial compression test	HR-9#	48.20	100.50	29.98
	HR-10#	48.30	99.30	27.66
	HR-11#	48.52	99.82	34.65
	HR-12#	48.52	99.24	31.63
	HR-13#	48.54	99.34	28.49

Creep tests: multi-level loading-unloading

Different from multi-level loading process, the stress was unloaded to zero after maintained for the creep time, and then it was reloaded to the next stress level until the final stage of the set stress was applied. During this process, the AE monitoring was again synchronized with the compression-creep test. The two loading methods used in the creep tests are shown in Fig. 3.

In the figures of this manuscript, the time of the creep test is defined as T_t; the axial strain of the specimen is defined as ε_1.

Comparison of acoustic emission amplitude of creep tests with two loading paths

The maximum amplitude of the AE waveform signal is referred to as the acoustic emission amplitude (AE amplitude). The relationships among AE amplitude, axial strain, and time for specimen HR-7# are shown in Fig. 4, and those for specimen HR-3# are shown in Fig. 5.

During the loading process, new internal cracks emerge and expand in the specimen after applying higher level of stress, and AE also behaves significantly. When a red sandstone specimen is subjected to creep test involving multi-level loading only, the frequency at which the AE amplitude changes is relatively high at low stress and decreases with the stress increases. When the stress reaches the rock creep threshold, both the alteration frequency and the AE amplitude increase, and the AE amplitude reaches its maximum when the specimen undergoes accelerated creep damage. The variation in AE amplitude reveals the damage evolution of the internal rock microstructure to a certain extent because the rock interior is dominated by the compaction of micro-cracks under the low stress. As the stress increases, the intrinsic cracks inside the rock expand and connect, their number decreases, and their scale increases. When the stress reaches the creep threshold, new internal cracks emerge and expand until to the macroscopic instability damage.

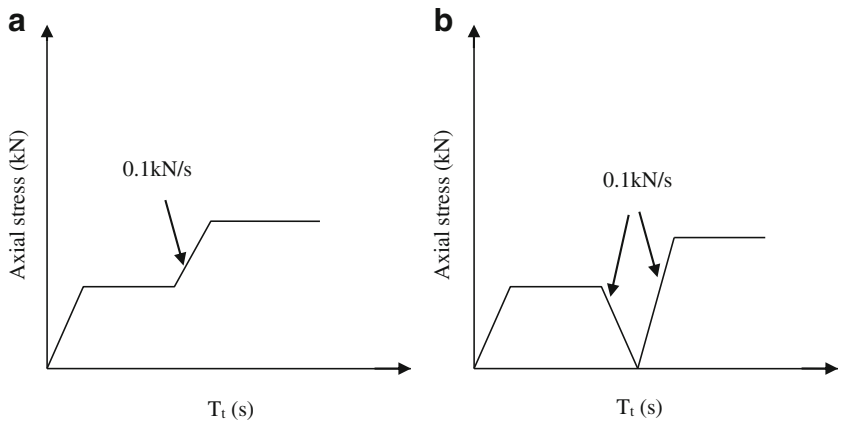

Fig. 3 Loading methods of creep test: (**a**) multi-level loading and (**b**) multi-level loading-unloading

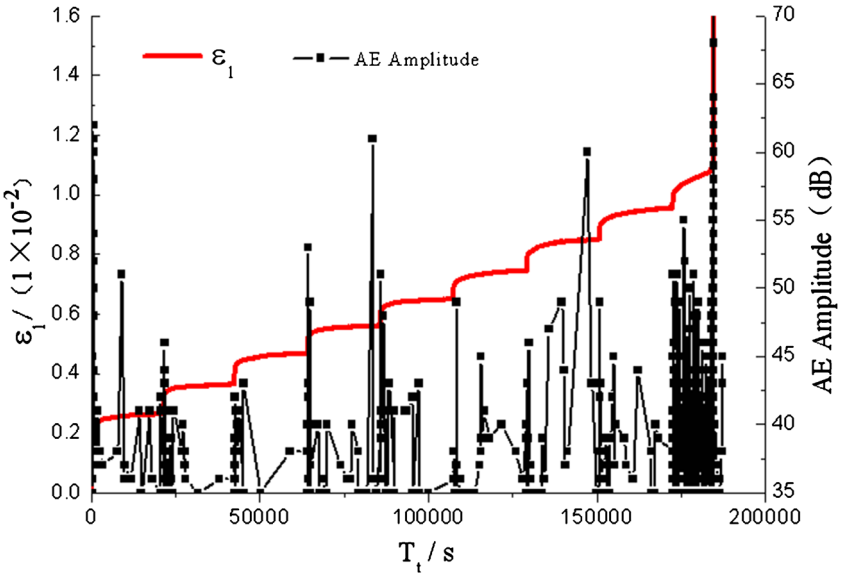

Fig. 4 Relationships among AE amplitude, axial strain, and time of multi-level loading creep test on specimen HR-7#

When a red sandstone specimen is subjected to creep test involving multi-level loading-unloading, its internal structure undergoes the compaction of the original cracks and pores and the emergence of new cracks under the low several stress levels. The AE activity is enhanced during the loading-unloading process at each stage but tends to weaken when the load is maintained. The AE amplitude decreases as the stress increases. Therefore, under low stress, the rock interior is dominated by crack compaction, and the loading process has little effect on the rock stability. Under higher stress, the internal damage evolution of the rock is dominated by crack propagation.

The variations of AE amplitude during the creep tests of the red sandstone specimen under two loading paths have similar characteristics: The AE amplitude of the rock under each stress-level creep condition exhibits the trend of "elevation → stationary → elevation." The AE amplitude decreases as the stress increases. However, the AE amplitude variation under these two loading paths is different: The alteration frequency and AE amplitude during the creep process involving multi-level loading-unloading are both significantly higher than those under multi-level loading.

Comparison of cumulative acoustic emission parameters of creep tests with two loading paths

Cumulative acoustic emission event

The number of AE event accumulated during the statistical time is called the cumulative AE event. The relationships among the cumulative AE event, axial strain, and time for

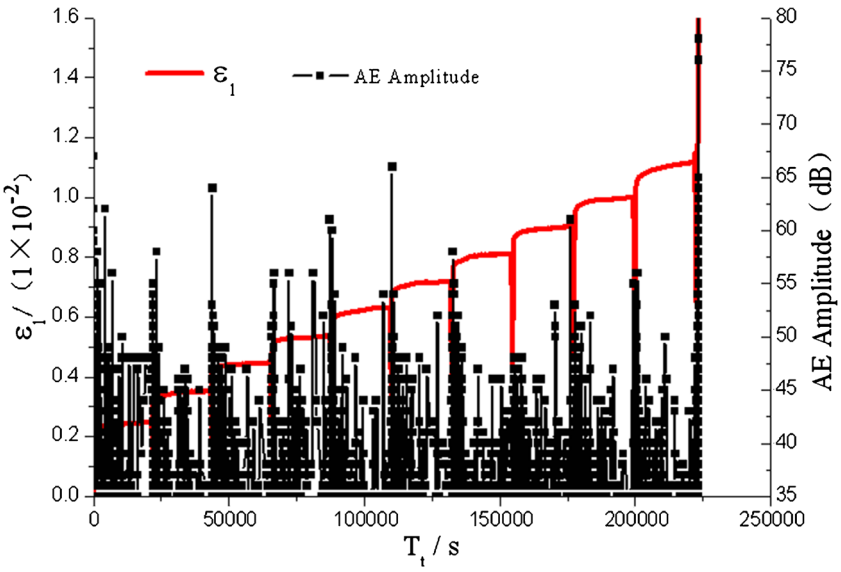

Fig. 5 Relationships among AE amplitude, axial strain, and time of multi-level loading-unloading creep test on specimen HR-3#

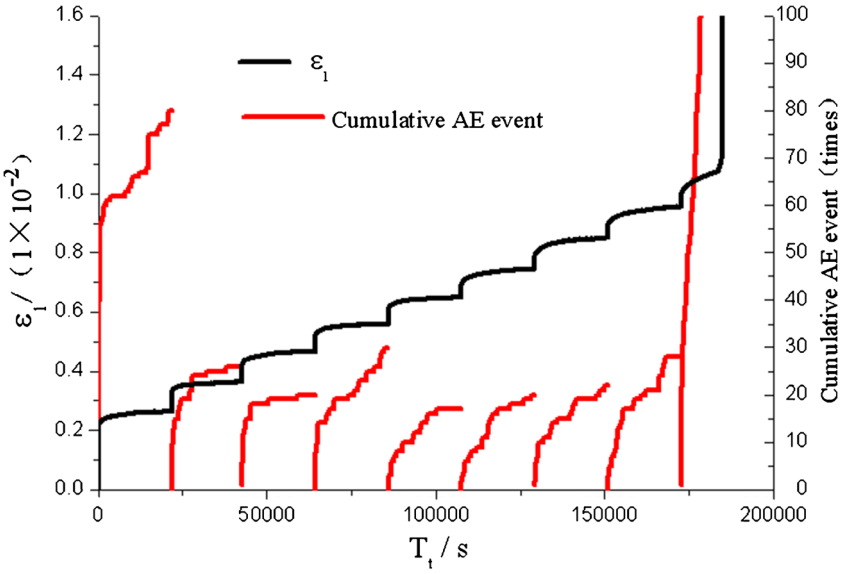

Fig. 6 Relationships among cumulative AE event, axial strain, and time of multi-level loading creep test on specimen HR-7#

specimen HR-7# are shown in Fig. 6, and those for specimen HR-3# are shown in Fig. 7.

When the red sandstone specimen is subjected to creep test under only multi-level loading, the cumulative AE event increases linearly with time during the first stress-level creep. The cumulative AE event exhibits an upwardly convex trend with increasing stress, and this trend becomes more obvious with a higher stress. While the curve appears to increase linearly once the stress reaches a certain value. This shows that under low stress, the AE activity inside the rock is more severe, and many rock cracks appear to be closed. As the stress increases, the AE activity weakens, and the original cracks inside the rock expand and connect. When the stress reaches a certain threshold, many new cracks in the rock are created and the AE activity is enhanced, which results in the cumulative AE event increasing.

When the red sandstone specimen is subjected to creep test under multi-level loading-unloading, the variation of the cumulative AE event with time in the creep process is similar to that under multi-level loading only, but the value is obviously higher.

Cumulative acoustic emission ring-down count

Acoustic emission ring-down count refers to the number of oscillations of the signal produced by it crossing the threshold voltage, and the number of acoustic emission ring-down count accumulated during the statistical time is called the cumulative AE ring-down count. The relationships among cumulative AE ring-down count, axial strain, and time for specimen HR-7# are shown in Fig. 8, and those for specimen HR-3# are shown in Fig. 9.

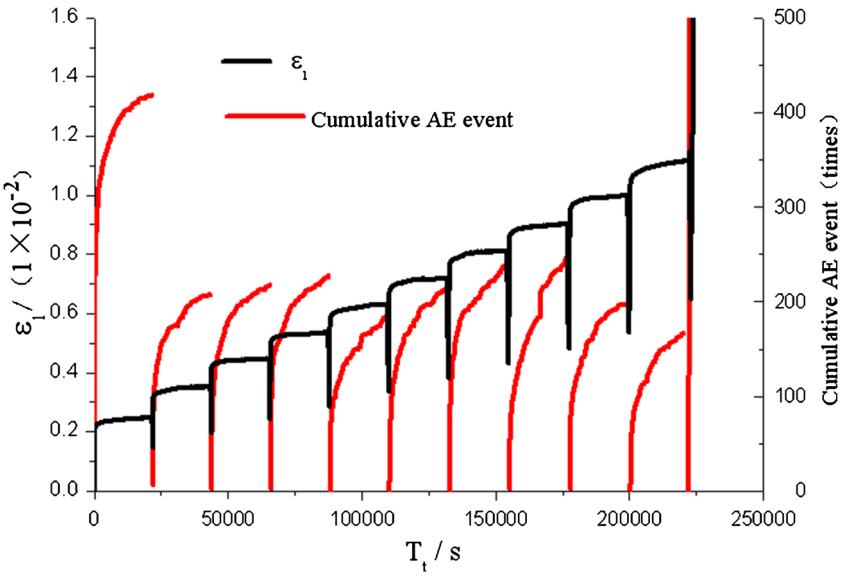

Fig. 7 Relationships among cumulative AE event, axial strain, and time of multi-level loading-unloading creep test on specimen HR-3#

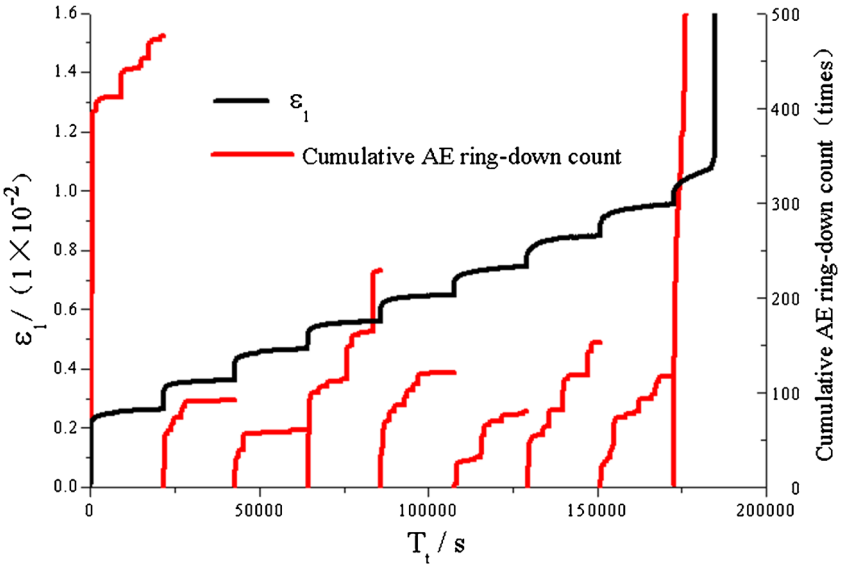

Fig. 8 Relationships among cumulative AE ring-down count, axial strain, and time of multi-level loading creep test on specimen HR-7#

When the red sandstone specimen is subjected to creep test under only multi-level loading, the cumulative AE ring-down count increases linearly with time at low stress levels. Then the cumulative AE ring-down count exhibits an upwardly convex trend with increasing stress, and the higher the stress, the more obvious that trend. When the stress reaches a certain value, the cumulative AE ring-down count appears to increase linearly with time. At the final stress level, the rock exhibits accelerated creep damage, and the cumulative AE ring-down count increases dramatically with time.

When the red sandstone specimen is subjected to creep test under multi-level loading-unloading, the variation of the cumulative AE ring-down count with time in the creep process is similar to that under multi-level loading only, while the value is obviously higher.

Damage variable for creep-AE characteristics of rock

Evolution of rock damage

Heterogeneous statistical description

Because the mesostructure of rock materials is highly random in shape, size, direction, and distribution, it is feasible to use statistical analysis to obtain a discrete description of the rock damage evolution. We choose a micro-body v in a heterogeneous rock sample, where v is deemed large enough to contain many micro-cracks and micro-pores and can therefore be regarded as a continuous medium. Under this premise, we introduce the following Weibull statistical distribution

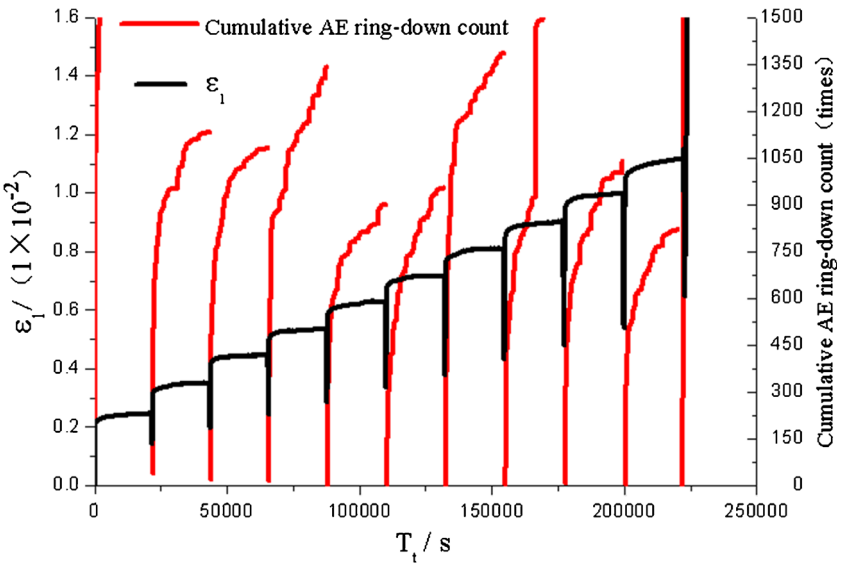

Fig. 9 Relationships among cumulative AE ring-down count, axial strain, and time of multi-level loading-unloading creep test on specimen HR-3#

Table 2 Results of theoretical model (Eq. (4)) characterizing the damage variable for specimen HR-7#

Load	10 kN	15 kN	20 kN	25 kN	30 kN	35 kN	40 kN	45 kN	50 kN	55 kN
Damage variable D	7.32%	0.21%	0.81%	0.49%	0.45%	1.39%	4.94%	5.12%	79.27%	

Table 3 Results of cumulative AE event characterizing the damage variable for specimen HR-7#

Load	10 kN	15 kN	20 kN	25 kN	30 kN	35 kN	40 kN	45 kN	50 kN	55 kN
Damage variable D	5.10%	0.45%	1.26%	1.08%	1.08%	1.84%	2.76%	3.11%	83.32%	

(Weibull 1951) to analyze the mechanical properties of this micro-body:

$$\varphi(a) = \frac{m}{a_0}\left(\frac{a}{a_0}\right)^{m\text{-}1} e^{-\left(\frac{a}{a_0}\right)^m} \tag{1}$$

where a is a mechanical parameter of the rock material (strain, elastic modulus, etc.), a_0 is the mean value of that mechanical parameter, m is the morphological parameter of the Weibull distribution function and reflects the homogeneity of the rock material, and $\varphi(a)$ is a statistical probability density function.

Damage evolution equation

The damage of the rock material is related to its internal micro-fracture structure. When the microstructure changes, the strength of the internal micro-body is affected; this can be expressed by the damage variable D and the probability density function of the microstructure damage in the form

$$\frac{dD}{d\varepsilon} = \varphi(\varepsilon) \tag{2}$$

where ε is the material strain of the rock.

From Eqs. (1) and (2), we obtain

$$\frac{dD}{d\varepsilon} = \varphi(\varepsilon) = \frac{m}{\varepsilon_0} \times \left(\frac{\varepsilon}{\varepsilon_0}\right)^{m\text{-}1} \times e^{-\left(\frac{\varepsilon}{\varepsilon_0}\right)^m} \tag{3}$$

And D is obtained by integrating Eq. (3), namely

$$D = \int_0^{\varepsilon}\varphi(x)dx = \int_0^{\varepsilon}\left(\frac{m}{\varepsilon_0}\left(\frac{x}{\varepsilon_0}\right)^{m\text{-}1} e^{-\left(\frac{x}{\varepsilon_0}\right)^m}\right)dx = 1\text{-}e^{-\left(\frac{\varepsilon}{\varepsilon_0}\right)^m} \tag{4}$$

Creep acoustic emission damage-variable model

In the present study, the damage variable is defined by the damage area, and the damage of the rock material is caused mainly by a reduction in the unit effective area. When establishing a creep AE damage-variable model, the following assumptions must be made.

1) There are a certain number of micro-defective micro-elements in any cross section of the specimen, and there is a certain difference in the intensity of each micro-element.
2) The intensity characteristics of the micro-element satisfy a Weibull statistical distribution.
3) Under the action of an external load, the rock specimen is evenly stressed and the strain is evenly distributed.

During the creep process of rock materials, the strain increases with time. The microstructure damages when its strain exceeds a certain value. Therefore, the damage area of the rock cross section can be expressed as (Tang and Xu 1990; Chen et al. 1997)

$$s = s_0\int_0^{\varepsilon}\varphi(x)dx \tag{5}$$

where s_0 is the cross-sectional area of the specimen in the initial (undamaged) state, $\varphi(x)$ is the intensity probability density function of the micro-body, and ε is the strain of the rock material.

According to Eq. (5), the damage variable D of the rock can be expressed as

$$D = s/s_0 = \int_0^{\varepsilon}\varphi(x)dx \tag{6}$$

Assuming that the cumulative AEs (AE ring-down count, AE event, etc.) generated by the damaged micro-element in unit cross-sectional area is n, the cumulative number ΔN of AEs generated within area ΔS can be expressed as

$$\Delta N = \mathrm{n} \times \Delta S \tag{7}$$

The cumulative AE N_{m} arises when the cross-sectional area S_0 of the rock specimen is completely destroyed, where upon Eq. (7) can be rewritten as

Table 4 Results of cumulative AE ring-down count characterizing the damage variable for specimen HR-7#

Load	10 kN	15 kN	20 kN	25 kN	30 kN	35 kN	40 kN	45 kN	50 kN	55 kN
Damage variable D	3.29%	0.25%	0.61%	0.41%	0.33%	1.03%	1.94%	2.11%	90.03%	

Table 5 Results of theoretical model (Eq. (4)) characterizing the damage variable for specimen HR-3#

Load	10 kN	15 kN	20 kN	25 kN	30 kN	35 kN	40 kN	45 kN	50 kN	55 kN	60 kN	65 kN
Damage variable D	7.34%	1.09%	1.12%	1.26%	1.67%	1.52%	2.05%	2.71%	5.37%	8.79%	67.08%	

$$\Delta N = \frac{N_m}{S_0} \times \Delta S \tag{8}$$

In the present study, we use strain as the variable of the statistical distribution. When the increment of axial strain of the specimen is $\Delta\varepsilon$ during the creep process, the increment of the corresponding damage area ΔS of the micro-element can be expressed as

$$\Delta S = S_0 \times \varphi(\varepsilon) \times \Delta\varepsilon \tag{9}$$

Substituting Eq. (9) into Eq. (8), we obtain

$$\Delta N/N_{\mathrm{m}} = \phi(\varepsilon)\cdot\Delta\varepsilon \tag{10}$$

During the creep deformation process, when the strain of the rock specimen increases to ε, the cumulative AE produced in the rock is

$$\Delta N = N_m\varphi(\varepsilon)\varepsilon = N_m\int_0^{\varepsilon}\varphi(x)dx \tag{11}$$

From Eqs. (6), (10), and (11), we obtain the following relationship between D and the number of AEs from the rock during the creep process:

$$D = \Delta N/N_m \tag{12}$$

Because the AEs from rock have a certain relationship with the damage variable of the rock, the variation of AE parameters can be used to evaluate the damage evolution of the rock.

ΔN_{i} (i = 1,2,….n) represents the cumulative AE generated during the creep process under stress level i, and N_m represents the sum of the cumulative AE during the creep process under each stress level.

Equations (5), (6), (7), (8), (9), (10), (11), and (12) are derived by Tang and Xu (1990) and Chen et al. (1997).

Verification and analysis of creep acoustic emission damage-variable model

We analyzed the test data of specimen HR-7# to study the applicability of the creep AE damage-variable model under the creep conditions of multi-level loading, which are presented in Tables 2, 3, and 4 and Fig. 10. And the applicability of the creep AE damage-variable model under the creep conditions of multi-level loading-unloading was also studied by using specimen HR-3#; those results are presented in Tables 5, 6, and 7 and Fig. 11.

According to analysis of the specimen subjected to multi-level loading, the results of the AE parameters characterizing the rock creep damage variable are consistent with those calculated by the theoretical model (Eq. (4)). Upon analyzing the specimen subjected to multi-level loading-unloading, although the rock creep damage variable characterized by AE parameters is different from that calculated by the theoretical model (Eq. (4)), the degree of disagreement is relatively small, and variation trend of the rock creep damage variable characterized by the theoretical model (Eq. (4)) is similar to that characterized by the creep AE model. Therefore, the creep AE damage-variable model could be used to characterize the evolution of rock damage during the creep process involving multi-level loading-unloading.

When the red sandstone specimen is subjected to creep test involving multi-level loading only, the damage variable exhibits a U-shaped distribution with stress. The damage variable is larger at low stress, smaller at medium stress, and larger once again at high stress. At low stress, the cracks and pores inside the rock are closed; thus, the damage variable is larger, but the damage in this stage has a limited effect on the stability of the rock. With increased stress, the major internal damage of rock is the expansion of the original crack. When the stress

Table 6 Results of cumulative AE event characterizing the damage variable for specimen HR-3#

Load	10 kN	15 kN	20 kN	25 kN	30 kN	35 kN	40 kN	45 kN	50 kN	55 kN	60 kN	65 kN
Damage variable D	9.64%	3.78%	3.96%	4.26%	4.22%	3.91%	3.92%	4.59%	5.49%	5.70%	50.53%	

Table 7 Results of cumulative AE ring-down count characterizing the damage variable for specimen HR-3#

Load	10 kN	15 kN	20 kN	25 kN	30 kN	35 kN	40 kN	45 kN	50 kN	55 kN	60 kN	65 kN
Damage variable D	5.42%	2.85%	2.72%	3.43%	2.30%	2.45%	2.24%	2.66%	3.54%	4.37%	67.82%	

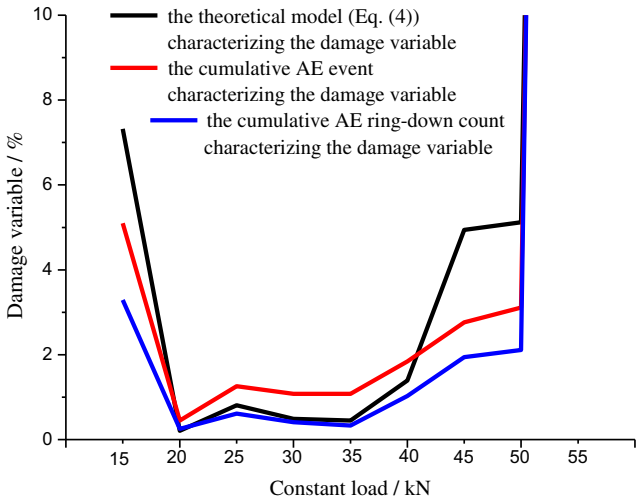

Fig. 10 Comparison of creep AE damage variables of creep test involving multi-level loading

reaches the creep threshold, the damage evolution of the rock is characterized by the expansion of new cracks leading to macroscopic instability failure; thus, the damage variable reaches its maximum.

When the red sandstone specimen is subjected to creep test involving multi-level loading-unloading, the variation of the damage variable is similar to that observed involving only multi-level loading.

Conclusions

Creep-AE tests on red sandstone specimens under only multi-level loading and multi-level loading-unloading were carried out, and some main conclusions are as follows:

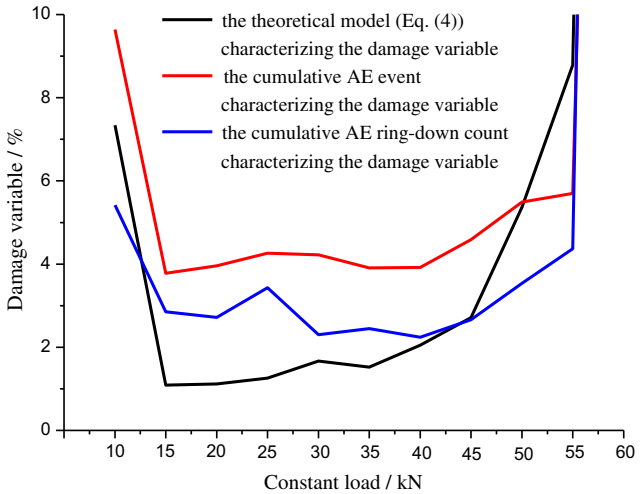

Fig. 11 Comparison of creep AE damage variables of creep test involving multi-level loading-unloading

(1) During the creep process involving multi-level loading-unloading, the temporal variation of AE amplitude is similar to that observed during the creep process involving only multi-level loading, and both exhibit a trend of "sudden increase ➞ stationary fluctuation ➞ sudden increase." However, the frequency of AE is significantly higher during the creep process involving multi-level loading-unloading.
(2) Under the previous stress levels, the temporal variations of the cumulative AE event and cumulative AE ring-down count during the creep process involving only multi-level loading are similar to those during the creep process involving multi-level loading-unloading.
(3) The creep AE damage-variable model could be used to characterize the damage evolution of the internal rock micro-crack structure during the creep process involving either only multi-level loading or multi-level loading-unloading.

Funding This work was supported by the National Natural Science Foundation of China (Grant Nos. 51064010 and 41002108) and the Systematic Project of Guangxi Key Laboratory of Disaster Prevention and Engineering Safety (Grant No. 2019ZDK051).

References

Chen ZH, Tang CA, Xu XH, Li CL (1997) Theoretical and experimental studies for Kaiser effect in rock. Chin J Nonferrous Metals 7:9–12 [In Chinese]

Hu B, Yang SQ, Xu P, Cheng JL (2019) Cyclic loading-unloading creep behavior of composite layered specimens. Acta Geophys 67:449–464

Huang X, Liu QS, Liu B, Liu XW, Pan YC, Liu JP (2017) Experimental study on the dilatancy and fracturing behavior of soft rock under unloading conditions. Int J Civ Eng 15:921–948

Kim JS, Lee KS, Cho WJ, Choi HJ, Cho GC (2015) A comparative evaluation of stress-strain and acoustic emission methods for quantitative damage assessments of brittle rock. Rock Mech Rock Eng 48:495–508

Kong XG, Wang EY, Li SG, Lin HF, Zhang ZB, Ju YQ (2020) Dynamic mechanical characteristics and fracture mechanism of gas-bearing coal based on SHPB experiments. Theor Appl Fract Mech 105: 102395

Meng QB, Zhang MW, Han LJ, Pu H, Chen YL (2016) Effects of acoustic emission and energy evolution of rock specimens under the uniaxial cyclic loading and unloading compression. Rock Mech Rock Eng 49:3873–3886

Meng QB, Zhang MW, Han LJ, Pu H, Chen YL (2018) Acoustic emission characteristic of red sandstone specimens under uniaxial cyclic loading and unloading compression. Rock Mech Rock Eng 51:969–988

Tang CA, Xu XH (1990) Evolution and propagation of material defects and Kaiser effect function. J Seismol Res 13:203–213 [In Chinese]

Wang QS, Chen JX, Guo JQ, Luo YB, Wang HY, Liu Q (2019) Acoustic emission characteristics and energy mechanism in karst limestone failure under uniaxial and triaxial compression. Bull Eng Geol Environ 78:1427–1442

Weibull W (1951) A statistical distribution function of wide applicability. J Appl Mech 18:293–297

Yang WD, Zhang QY, Li SC, Wang SG (2014a) Estimation of in situ viscoelastic parameters of a weak rock layer by time-dependent plate-loading tests. Int J Rock Mech Min Sci 66:169–176

Yang SQ, Ni HM, Wen S (2014b) Spatial acoustic emission evolution of red sandstone during multi-stage triaxial deformation. J Cent South Univ 21:3316–3326

Yang SQ, Xu P, Ranjith PG, Chen GF, Jing HW (2015) Evaluation of creep mechanical behavior of deep-buried marble under triaxial cyclic loading. Arab J Geosci 8:6567–6582

Zhang ZP, Zhang R, Xie HP, Liu JF, Were P (2015) Differences in the acoustic emission characteristics of rock salt compared with granite and marble during the damage evolution process. Environ Earth Sci 73:6987–6999

Zhang J, Ai C, Li YW, Che MG, Gao R, Zeng J (2018) Energy-based brittleness index and acoustic emission characteristics of anisotropic coal under triaxial stress condition. Rock Mech Rock Eng 51:3343–3360

Zhao YL, Cao P, Wang WJ, Wan W, Liu YK (2009) Viscoelasto-plastic rheological experiment under circular increment step load and unload and nonlinear creep model of soft rocks. J Cent S Univ Technol 16:0488–0494

Zhao YL, Zhang LY, Wang WJ, Wan W, Li SQ, Ma WH, Wang YX (2017a) Creep behavior of intact and cracked limestone under multi-level loading and unloading cycles. Rock Mech Rock Eng 50:1409–1424

Zhao YL, Wang YX, Wang WJ, Wan W, Tang JZ (2017b) Modeling of non-linear rheological behavior of hard rock using triaxial rheological experiment. Int J Rock Mech Min Sci 93:66–75